**Keller, N.-S.**, Hornbruch, G., Lüders, K., **Werban, U.**, **Vogt, C.**, **Kallies, R.**, Dahmke, A., **Richnow, H.H.** (2021):
Monitoring of the effects of a temporally limited heat stress on microbial communities in a shallow aquifer
*Sci. Total Environ.* **781** , art. 146377

# Monitoring of the effects of a temporally limited heat stress on microbial communities in a shallow aquifer

Nina Sophie Keller[a], Götz Hornbruch[b], Klas Lüders[b], Ulrike Werban[c], Carsten Vogt[a], René Kallies[d], Andreas Dahmke[b], & Hans Hermann Richnow[a]

[a]Helmholtz Centre for Environmental Research – UFZ, Department of Isotope Biogeochemistry, 04318 Leipzig, Germany (nina-sophie.keller@ufz.de; carsten.vogt@ufz.de; hans.richnow@ufz.de)

[b]University of Kiel, Institute for Geosciences, 24118 Kiel, Germany (goetz.hornbruch@ifg.uni-kiel.de; klas.lueders@ifg.uni-kiel.de; andreas.dahmke@ifg.uni-kiel.de)

[c]Helmholtz Centre for Environmental Research – UFZ, Department Monitoring & Exploration Technologies, 04318 Leipzig, Germany (ulrike.werban@ufz.de)

[d]Helmholtz Centre for Environmental Research – UFZ, Department Environmental Microbiology, 04318 Leipzig, Germany (rene.kallies@ufz.de)

**Corresponding author:**

Carsten Vogt (+49 341 235 1357; carsten.vogt@ufz.de)

# Highlights

- Emulation of the initial operating phase of the affected space of a HT-ATES system with a short-term infiltration of warm water into a porous middle European aquifer
- A moderate increase (< 35 °C) of the groundwater temperature (9 ± 2 °C) did not significantly influence the compositions of the microbial groundwater communities and the total number of cells
- The results indicate that the groundwater microbiome was resilient to the temporally limited heat stress

Graphical Abstract

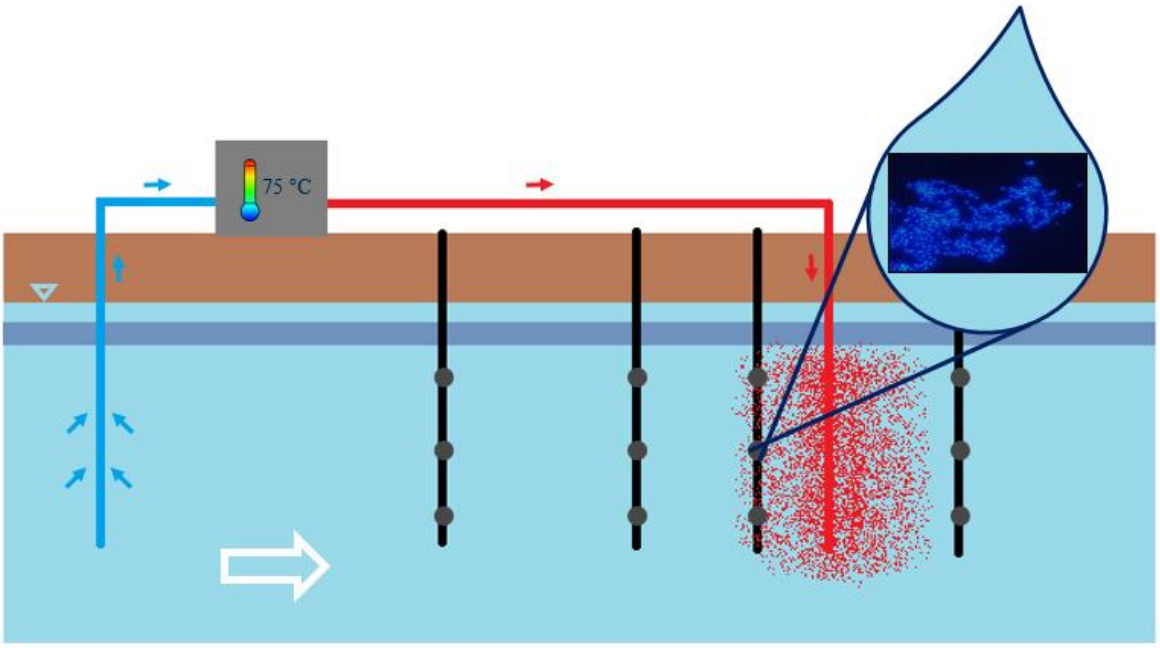

## Abstract

Aquifer thermal energy storage (ATES) is a key concept for the use of renewable energy resources. Interest in ATES performed at high temperature (HT-ATES; > 60 °C) is increasing due to higher energetic efficiencies. HT-ATES induces temperature fluctuations that exceed the natural variability in shallow aquifers, which could lead to adverse effects in subsurface ecosystems by altering the groundwater chemistry, biodiversity, and microbial metabolic activity, resulting in changes of the groundwater quality, biogeochemical processes, and ecosystem functions. The aim of this study was to emulate the initial operating phase of a HT-ATES system with a short-term infiltration of warm water into a Pleistocene sandur sediment and, consequently, to monitor the thermal effects on the groundwater biome inhabiting an imitated affected space of an HT-ATES system. Therefore, local groundwater was withdrawn, heated up to 75 °C, and re-infiltrated into a shallow aquifer located near Wittstock/Dosse (Brandenburg, Germany) for around five days. Groundwater samples taken regularly before and after the infiltration were analyzed by 16S rRNA gene amplicon sequencing for microbial diversity analyses as well as total cell counting. During the infiltration, a thermal plume with groundwater temperatures increasing from 9 ± 2 to up to ~ 65 °C was recorded. The highest temperature at which groundwater samples were taken was 34.9 °C, a temperature typically arising in the affected space of an HT-ATES system. The microbial communities in the groundwater were mainly composed of *Gammaproteobacteria*, *Alphaproteobacteria*, *Bacteroidia*, and *Actinobacteria*, and the total cell numbers ranged from $3.2 * 10^4$ to $3.1 * 10^6$ cells $ml^{-1}$. Neither the compositions of the microbial communities nor the total number of cells in groundwater were significantly changed upon moderate temperature increase, indicating that the diverse groundwater microbiome was resilient to the temporally limited heat stress.



## Keywords

46 Heat stress, temperature, ATES, shallow aquifer, groundwater, microbial community, amplicon
47 sequencing

## 1. Introduction

The necessary reduction of energy consumption from fossil fuels and a rising power demand of society for heating and cooling require cost-efficient options for the temporal storage of thermal energy in the subsurface, also to compensate seasonal mismatches between energy demand and supply. In underground thermal energy storage (UTES), the natural subsurface is used sustainably for the periodical storage of thermal energy (Novo et al., 2010), whereat, the stored energy can later be used for space heating and cooling (Lee, 2010). The conjunction of production and consumption patterns by using excess heat from industrial production, cooling, and other processes for saving waste heat for warming of buildings in cold seasons may save electricity and also fossil fuels (Fleuchaus et al., 2018). This could contribute to a reduction of greenhouse gas emissions, such as $CO_2$, $SO_x$, and $NO_x$, to the atmosphere (Novo et al., 2010). Aquifer thermal energy storage (ATES) is one concept for UTES (Novo et al., 2010), where groundwater from a saturated and permeable underground layer is used directly for both heating and cooling purposes at different periods of the year, either in continuous or cyclic regime, with spatially separated but hydraulically-coupled wells for water extraction and infiltration (Lee, 2010). More than 2800 ATES systems have been successfully applied all over the world, mainly in urban and agricultural areas for heating and/or cooling of residential, commercial, public, and industrial buildings as well as greenhouses. Of these, 85% are located in the Netherlands and 99% operate in a low-temperature range of < 25 ºC (Fleuchaus et al., 2018), as 20 – 25 °C is the accepted infiltration temperature limit for open geothermal systems in some European countries (Hähnlein et al., 2011). While strategies have been developed for the optimization of ATES design to improve efficiency (Sommer et al., 2015), interest in high-temperature ATES (HT-ATES) applications is increasing because the energy density per volume of water is higher. HT-ATES systems can be operated with temperatures above 60 °C, lowering the energy needed for a heat pump to adjust to the target temperature, which improves energy savings, and a lower

flow rate can be applied due to the higher energy level per cubic meter of water (Drijver et al., 2012).

In the subsurface, ATES systems induce temperature changes that exceed the natural fluctuations (Drijver et al., 2012). Notably, the operational space, i. e., the actual subsurface storage area with retrievable cold/heat, has a much smaller spatial expansion than the subsequently entailed affected space after a certain operating time of the system. ATES hereby causes thermal, hydraulic, and (bio-) chemical alterations in the aquifer outside the area where groundwater is actively utilized (Figure A.1). In regard to heat storage, the thermal effects are much lower in the affected space compared to the operational space (Dahmke et al., 2020), specifically, around 30°C (affected space) and 90°C (operational space) (Degenhart et al., 2019). Whereas, the natural groundwater temperature in 10 – 20 m depth is around 8 – 14 °C in Germany throughout the year (Griebler & Avramov, 2015) without significant seasonal variability. Previous studies showed that an increase in temperature in aquifers leads to the mobilization of organic matter (OM) and some trace elements, particularly at temperatures above 60 °C (Brons et al., 1991; Christ & David, 1996; Kaiser et al., 2001; Bonte et al., 2011; Bonte et al., 2013a; Bonte et al., 2013b; Jesußek et al., 2013a; Lüders et al., 2020), a lower solubility of gases (Jenne et al., 1992; Lüders et al., 2016), a decrease in pH (Brons et al., 1991; Jesußek et al., 2013a), and an increased dissolution or precipitation of major elements (Palmer & Cherry, 1984; Holm et al., 1987; Griffioen & Appelo, 1993; Arning et al., 2006; Jesußek et al., 2013a: Bonte et al., 2013b). Groundwater ecosystems are considered as vulnerable systems associated with low resistance and weak resilience against environmental disturbance, such as temperature changes, since they are predominantly in a steady-state and usually oligotrophic, i. e., low in biodegradable carbon, nutrients, and energy (Griebler et al., 2016).

Thriving in almost constant thermal environmental conditions, the organisms in groundwater might as well be sensitive and not very tolerant against thermal disturbances (Griebler & Avramov, 2015; Griebler et al., 2016). In groundwater in Germany, the microbial communities

99 are mainly composed of psychrophilic and psychrotolerant prokaryotes (Griebler et al., 2016);
100 generally, these microorganisms perform ecosystem services, such as the purification of water,
101 the biodegradation of pollutants, the inactivation/elimination of pathogens, as well as carbon
102 and nutrient cycling (Griebler & Avramov, 2015). The temperature ranges for the growth of
103 psychrophilic and psychrotolerant prokaryotes are between -5 – 18 °C and -2 – 35 °C,
104 respectively. The typical thermal growth conditions for mesophiles (15 – 44 °C) and
105 thermophiles (42 – 79 °C) (Reineke & Schlömann, 2015) are usually not realized in natural
106 German aquifers. With a rise in temperature into the specific growth range, the growth and
107 activity of microorganisms from certain groups are expected to be stimulated, especially around
108 the optimal growth temperature. Several studies investigated temperature effects on the
109 microbial diversity on the laboratory scale, showing significant changes both at moderate (Zogg
110 et al., 1997; Bradford et al., 2008; Yergeau et al., 2012) and high (≥ 45 °C) (Bonte et al., 2013a;
111 Bonte et al., 2013b; Metze et al., 2020) temperature increases. Generally, alterations towards
112 (stronger) reducing conditions (Jesußek et al., 2013a; Jesußek et al., 2013b; Griebler et al.,
113 2016) and subsequent changes in the diversity and composition of the microbial communities
114 have been demonstrated (Bonte et al., 2013a; Griebler et al., 2016). Major shifts occurred
115 mainly in case of chronic heat exposures and at temperatures ≥ 45 °C. Recently, we examined
116 thermal effects on the microbial diversity and activity in controlled laboratory microcosm
117 experiments using Pleistocene sandur sediment and groundwater from a shallow aquifer near
118 Wittstock/Dosse (Brandenburg, Germany); the community did not alter when incubated at 12,
119 25, and 37 °C, but significantly changed at incubation temperatures of 45 and 60 °C (Metze et
120 al., 2020). Regarding field investigations, however, a very limited number of studies examining
121 temperature effects on the microbial diversity and abundance in near-surface aquifers is
122 available. A weak but significant positive correlation between bacterial diversity and
123 temperature and, respectively, no temperature effect on the total bacterial cell counts were

shown in an oligotrophic shallow aquifer impacted by a heat plume (≤ 21 °C) from a facility's discharge (Brielmann et al., 2009).

In this study, we aimed to monitor the effects of a heat stress on the microbial communities in a short-term in situ experiment at the field site near Wittstock/Dosse (Brandenburg, Germany). Groundwater was withdrawn, heated up to 75 °C, and re-infiltrated on a filter stretch from 7 – 14 m below ground surface (bgs) into an aquifer for about 5 days, in order to emulate the initial operating phase of a HT-ATES system. We focus on investigating the thermal effects in the - consequently imitated - space after groundwater cooling, as the affected space entailed by heat storage of a HT-ATES system. Changes in the microbial community composition in the operational space will be investigated in future field experiments. Using groundwater samples, the effects on the composition of the microbial communities inhabiting the aquifer were monitored with 16S rRNA gene amplicon sequencing and total cell counting. To our knowledge, this is the first study applying these methods to investigate the effects of a heat stress on microorganisms in a field experiment. We hypothesize that the composition of the microbial communities' shifts due to the heating, as the conditions might be most favorable for mesophilic microorganisms, and the number of cells might slightly increase because of higher DOC availability and rising microbial metabolic activity.

## 2. Material and Methods

### 2.1 Field site, infiltration test, and groundwater sampling

The infiltration experiment was conducted on a field site near Wittstock/Dosse (Brandenburg, Germany), located about 100 km North of Berlin. The subsurface is composed of typical Quaternary sediments from the Pleistocene age, including sandur deposits. The unsaturated soil zone consists of sand as well as silt and the water table is located about 3 m bgs. Two mainly confined aquifers (gfW1n-2v and gfS1n-2v) were detected, consisting of fine to coarse sands, silt, clay, and glacial loam of the Saale and Vistula ice age, respectively. Aquifer 1 (up to 5 – 6

m bgs) is characterized by heterogeneously distributed interbedded sand and silt layers and aquifer 2 extends to a depth of about 15 – 16 m in this part of the field site (Hornbruch et al., in prep.). A discontinuous confining layer made of glacial loam (gS-II) with variable thickness partly separates these. Hydraulic connections between the aquifers were shown by direct push-driven hydraulic profiling tool (HPT) logs (Geoprobe Systems, Salina, Kansas) and piezometric measurements. Glacial till makes up the aquitard at the lower basis (Peter et al., 2011). This till layer is dipping from East to West and was detected in some locations at depths between about 15 and 22 m by drilling samples and HPT logs. The groundwater flows in West-South-West direction with an average velocity of 5 cm/d. Hydraulic conductivity is in the range of 3E-4 m/s. In sampling well D09, for example, the temperature profiles in 1 m depth showed fluctuation between about 4 °C (November 2018) and 14 °C (May 2019), while in 7 m depth (top of the filter screen of the infiltration well), the measured temperature range decreased to 9 – 11 °C, and a mean temperature of about 10 ± 1°C was detected in 17 m bgs. Prior to the infiltration experiment, the hydrochemistry of the aquifer was characterized (Table A.1).

In May 2019, 86 m³ of groundwater were withdrawn from a 2" well (sonic drilling), heated up to around 75 °C using a commercial heat exchanger (WZ 150 kW and FWM 140KW, Heizkurier GmbH, Wachtberg, Germany), and gravitationally re-infiltrated into a 2" well (sonic drilling) located 40 m downstream of the extraction well with an infiltration rate of about 14.5 L/min on a filter stretch from 7 – 14 m bgs for around five days. The infiltration horizon was chosen due to the relatively homogeneous composition of the aquifer from ~ 6 – 15 m depth, as derived from HPT logs. Continuous temperature measurements were conducted utilizing thermocouples (Type T PFA Insulated Flat Pair Thermocouples, Labfacility Ltd., Dinnington, England) that were attached outside of the high-density polyethylene (HDPE) tubes (Eijkelkamp Soil & Water, Giesbeek, The Netherlands, or Solinst©/Canada for CMT-system, UTK-EcoSense GmbH, Zeitz, Germany) during installation directly next to the sampling depths

as well as over the entire aquifer depth (ten temperature measurements in total for each well at 1, 2, 4, 5, 6.5, 7.5, 9, 10.5, 13.5, and 17 m bgs).

Groundwater was sampled from 2" wells (U00 [extraction well], U15, U07, U01, C06 [infiltration well], C10, and D09; Figure 1) during eight field campaigns utilizing submersible pumps (MP1, Grundfos GmbH, Erkrath, Germany, or Whale submersible electric galley pump, Munster Simms Engineering Ltd., Bangor, Northern Ireland) with low pumping rates of 3 – 5 L/min to minimize hydraulic effects and perturbation of hydrogeochemical stratification. Four samplings took place before the infiltration in October, November, and December 2018 as well as in April 2019 and four after the infiltration in the period from June to the end of July 2019 (two samplings per month; 7, 27 – 28, 40 – 43, and 62 – 63 days after the infiltration, respectively). In October and November 2018, integral sampling was carried out, whereas, the groundwater was taken locally at the discrete depths of 7.5 m, 10.5 m, and 13.5 m from December 2018 onwards. For each sample for diversity analysis (see section 2.2), 4 liters of groundwater were filled into four sterilized 1-liter Schott serum bottles. In addition, 5 ml of groundwater were taken for total cell counting (see section 2.3). The samples were fixed on site with 5 ml of 4% paraformaldehyde (PFA) in a sterilized 50 ml serum bottle which was sealed with butyl rubber stoppers and aluminum crimp seals. The 4% PFA had been prepared by mixing 16% PFA aqueous solution (Electron Microscopy Sciences, Pennsylvania, USA) 1:4 with 10-fold diluted PBS buffer (Phosphate-Buffered Saline (10X), RNase-free buffer adjusted to pH 7.4; Thermo Fisher Scientific, Waltham, MA, USA). All samples were stored in a fridge afield for 1 to 3 days and subsequently transported cooled to the Helmholtz Center for Environmental Research (UFZ) in Leipzig and processed within one week.

## 2.2 Analyses of groundwater microbial communities by 16S rRNA gene amplicon sequencing

Prior to 16S rRNA gene amplicon sequencing, each 4-liter sample was filtered through a sterile 0.22 µm S-Pak filter (Merck, Darmstadt, Germany) and, afterwards, through a sterilized 0.1 µm hydrophilic PES membrane filter (Sartorius™, Goettingen, Germany), in order to also capture ultra-small microorganisms. For filtration, an all-glass vacuum filter holder system for 47 mm membrane filters (Sartorius™, Goettingen, Germany) connected to a diaphragm vacuum pump (Sartorius™, Goettingen, Germany, or KNF Neuberger, Freiburg im Breisgau, Germany) was used. The filters were either stored in sterile 50 ml Falcon tubes (Centrifuge Tube 50 ml, PP, Th. Geyer GmbH & Co. KG, Renningen, Germany) at -20 °C until further processing or the DNA was extracted immediately after the filtration. The DNA was extracted individually from the filters using the DNeasy PowerWater Kit (QIAGEN, Germantown, MD, USA) according to the manufacturer's instructions. The concentration and the purity of DNA were measured utilizing a NanoDrop 2000 (Thermo Fisher Scientific, Waltham, MA, USA). The DNA extracted from the 0.22 µm filter and the 0.1 µm filter was mixed 1:1 (vol:vol) for the amplicon sequencing and stored at -20 °C.

To amplify the V3 – V4 rRNA region (444 base pairs [bp]), a two-step, tailed PCR approach that generates ready-to-pool amplicon libraries was conducted. The PCR was performed as described by Klindworth and colleagues (2013) using a 2x MyTaq™ Mix (Bioline, Heidelberg, Germany). The primer pair, 341-F and 785-R, was chosen due to the good coverage of bacterial diversity (Klindworth et al., 2013). Sequencing libraries were prepared according to the Illumina 16S Metagenomic Sequencing Library Preparation protocol and the 4 nM pooled library was run on an Illumina MiSeq system (Illumina, California, USA) using the V3 600 cycles chemistry.

The de-multiplexed raw sequence data was processed using QIIME2 2019.4 (Bolyen et al., 2019). Firstly, the primer sequences were removed and untrimmed reads as well as reads with a length <50 bp were discarded with cutadapt (Martin, 2011). DADA2, which is already implemented in QIIME2, was used for denoising, i. e., quality-filtering and quality-trimming, learning of the error rates, dereplicating, inferencing of the samples, merging of paired end reads, and removal of chimeras (Callahan et al., 2016a). The forward and the reverse reads were trimmed to 270 bp (--p-trunc-len-f 270) and 240 bp (--p-trunc-len-r 240), respectively. The SILVA v128 dataset, which is typically used to assign 16S sequences, was used for the taxonomic assignment and non-bacterial sequencing reads were removed from the dataset. Finally, sequences that could not be taxonomically assigned at the phylum level were removed due to their high probability of being sequence artifacts (Callahan et al., 2016b). Illumina MiSeq paired-end reads were deposited in the European Nucleotide Archive (ENA) under accession number PRJEB41454.

### 2.3 Total cell counting

The 5 ml groundwater samples fixed with 5 ml 4% PFA in the field were filtered through sterilized 0.1 µm pore size (hydrophilic polycarbonate membrane, 47 mm diameter) Isopore Membrane Filters (Merck, Darmstadt, Germany) utilizing the all-glass vacuum filter holder system connected to one of the vacuum pumps mentioned in section 2.2. Next, 5 ml each of 1x PBS buffer, 30%, 50%, 70%, and 80% aqueous ethanol solution were flushed through the same filter to wash out the PFA stepwise. Three pieces were cut out of every filter and incubated in 1 µg/ml 4′,6-diamidin-2-phenylindol dihydrochloride (DAPI; Thermo Fisher Scientific, Waltham, MA, USA) solution in the dark at RT for 10 – 15 minutes. The filter pieces were rinsed in sterilized MiliQ water and dipped into 80% ethanol. After drying, Citifluor vectashield (CV; CitiFluor™ AF1, Mounting Medium [Science Services GmbH, München, Germany] mixed 4:1 with Vectashield® Mounting Medium [LINARIS Biologische Produkte GmbH,

Dossenheim, Germany]) was placed on a microscopic glass plate, the filter pieces are added and covered with a glass cover slip. The samples were stored at -20 °C. Four pictures per filter piece were taken using an Imager.Z2 microscope (Carl Zeiss Microscopy GmbH, Jena, Germany) with 100x magnification. Cells were counted manually utilizing ImageJ 1.48v and the average number of cells per ml sample as well as the standard deviation were calculated.

### 2.4 Statistical analyses

Plotting and statistical analyses were performed utilizing RStudio version 1.3.1093 (RStudio Team, 2020). Compiled QIIME2 level 5 results (relative abundances > 5%) in samples from the baseline monitoring were compared to those in depth-specific samples from the heat effected wells taken post-infiltration to illustrate potential changes in the microbial diversity. First, the respective data frame was converted into a single column format with the *melt()* function (*reshape2* package; Wickham, 2007) and, then, the results were plotted using the function *ggplot()* (*ggplot2*: Wickham, 2016) and *ggpubr* packages (Kassambara, 2020a). Moreover, Friedman tests were performed to test if there is are significant differences between the baseline monitoring and the post-infiltration depth-specific samplings of heat effected wells. For the baseline data set, mean relative abundances were calculated (values for samples from the other wells at the different depths taken post-infiltration were used individually). Again, the respective data frame was gathered into a single column format. Next, a Friedman test was performed using the function *friedman_test()* (*rstatix* package; Kassambara, 2020b). Post-hoc, multiple pairwise comparisons (to check between which samplings potential differences occur) were done with a Wilcoxon signed-rank test using the function *wilcox_test()* (*rstatix* package; *bonferroni p.adjust.method*). The results were plotted utilizing *ggboxplot()* (*ggplot2*, *ggpubr*, and *tidyverse* (Wickham et al., 2019) packages.

The alpha diversity (here: Shannon-Wiener indices) was calculated for all samples (baseline data as wells as post-infiltration samples from all wells) using the function *diversity* (*vegan*

package (Oksanen et al., 2020); *shannon* index). These results were correlated versus the temperature with the function *cor.test* (*Kendall* method; *stats* package; R Core Team, 2020), after the data had been tested for a normal distribution and a homogeneity of the variances using the functions *shapiro.test* (*stats* package) and *leveneTest* (*car* package; Fox & Weisberg, 2019). The results were plotted with *ggplot()* (*ggplot2*, *dplyr* (Wickham et al., 2020), *patchwork* (Pedersen, 2020), *hrbrthemes* (Rudis, 2020), and *ggpubr* packages) and *ggarrange()* (*ggpubr* package). Furthermore, non-metric multidimensional scaling (NMDS) (Faith et al., 1987; Kruskal, 1964a; Kruskal, 1964b; Minchin, 1987), a distance-based ordination, was conducted for all samples to illustrate similarities/dissimilarities between different temperatures (beta diversity). At first, the function *vegdist()* (*vegan* package; *bray* method) was used to create a Bray-Curtis distance matrix of the double square root transformed QIIME2 level 5 results (relative abundances). The transformation was done in order to reduce the stress and the weight of the dominant taxa. The NMDS was conducted utilizing the function *metaMDS()* (*vegan* package) and plotted under the use of *ggplot()* (*ggplot2* package) and, respectively, the functions *ordiplot(), ordispider(),* and *ordihull()* (*vegan* package). For *ggplot(),* groups were created for samples that were taken at ambient (7 – 11 °C), medium (12 – 19 °C), and high (20 – 35 °C) groundwater temperatures. Next, a permutational analysis of variance (PERMANOVA) and a permutation test were conducted for all samples (Anderson, 2001; Anderson & Walsh, 2013); the PERMANOVA shows if the microbial communities statistically significantly differ between samplings at different temperatures and how much of the variance can be explained by a parameter (here: temperature), while the permutation test gives additional information on the dispersion within groups. With the function *adonis()* (*vegan* package; *bray* method), the PERMANOVA was performed on the double square root transformed QIIME2 level 5 results (relative abundances), and the permutation test was conducted using the functions *betadisper()* and *permutest()* (*vegan* package).

To test if there is a difference between the abundances of *Thermodesulfovibrionia* in samples taken before and after the infiltration, t-tests were performed using the function *t.test* (*stats* package), after the data had been tested for a normal distribution and a homogeneity of the variances using the functions *shapiro.test* (*stats* package) and *leveneTest* (*car* package), respectively. The relative abundance (> 5%; QIIME2 level 5) of *Thermodesulfovibrionia* were correlated versus the temperature utilizing function *cor.test* (*Kendall* method; *stats* package). Furthermore, the QIIME2 level 5 results (relative abundances) were correlated versus the temperature and taxa with correlation coefficients < -0.4 and > 0.4 were plotted with the function *ggplot()* (*ggplot2* package).

For a correlation against the temperature, the results of the total cell counts were tested in advance for a normal distribution and a homogeneity of the variances using the functions *shapiro.test* (*stats* package) and *leveneTest* (*car* package). The function *cor.test* (*Kendall* method; *stats* package) was used to correlate the values and the function *ggplot* (*ggplot2* package) to plot the results.

## 3. Results

During the infiltration, the temperature increased to a maximum of ~ 61 to 67 °C at the sampling depths (7.5, 10.5, and 13.5 m bgs) in well U01 (Table A.2), i. e., the most heat-influenced 2" well that was sampled, and cooled down to ~ 30 – 50 °C when the infiltration was terminated and to ~ 19 – 35 °C until the first sampling (9 and 7 days after the maximum temperature was recorded and, respectively, the end of the infiltration of heated groundwater). The previously heated groundwater flew through well D09, which showed slightly increased temperatures of 13 – 15 °C 62 - 63 days after the infiltration (see Table A.3). Since the wells U07 and C10 were not directly influenced by the heating, these were also considered as reference wells, besides well U15.

### 3.1 Microbial diversity in heat-influenced and non-heat-influenced parts of the aquifer

The most frequently occurring (assigned) microorganisms in the groundwater microbiome belonged to *Gammaproteobacteria* (especially *Burkholderiaceae* and *Pseudomonadaceae*), *Alphaproteobacteria* (especially *Sphingomonadaceae),* *Bacteroidia* (especially *Flavobacteriaceae*), and *Actinobacteria* (especially *Nocardiaceae*). *Campylobacteria* (*Thiovulaceae*), *Parcubacteria*, and *Omnitrophicaeota* were often represented as well. *Chloroflexi* (*KD4-96*), *Elusimicrobia* (*Lineage IV*), *Clostridia* (*Clostridiales Family XVIII*), *Latescibacteria*, *Nitrospirae* (*4-29-1*), *Thermodesulfovibrionia*, *Berkelbacteria*, *Brocadiae* (*Brocadiaceae*), and *Deltaproteobacteria* (*DTB120* and *Desulfobacteraceae*) were also recorded with a relative abundance of > 5% (QIIME 2 level 5) in at least one sample. Other microorganisms made up 0.6 – 60% of the microbial community (Figures 2 – 5 and A.2 – A.4); of these, some were *Dehalococcoidia*. At the QIIME2 level 3, 12.9% *Dehalococcoidia* were detected in the microbial community in sample 1812_U15_13.5 (data not shown).

In the heat-influenced wells U01 and D09, the compositions of the microbial communities detected after the infiltration were generally similar to the ones determined in samples from the baseline monitoring (Figures 2 – 5). The Friedman tests and Wilcoxon signed-rank tests performed post hoc confirmed that the microbial communities sampled post-infiltration from wells U01 and D09 (7.5 and 10.5 m bgs each) did not differ significantly from the baseline samples, except for sample 1907-2_U01_7.5 (Figure 6). However, statistically significant differences occurred in well D09 between samples taken at 7.5 m depth 27 – 28 and 40 – 43 days after the infiltration as well as between samples taken at 10.5 m depth 27 – 28, 40 – 43, and 62 – 63 days post-infiltration (Figure 6 C and D). In contrast, larger shifts in the microbial community compositions occurred in the reference wells U15, U07, and C10 (Figures A.2 – A.4). Friedman tests and subsequent Wilcoxon signed-rank tests additionally showed that the microbial communities sampled in wells U15, U07, and C10 each 10.5 m bgs differed between

samplings (U15; Figure A.5) as well as compared to the baseline samples and between samplings (C10 and U07; Figure A.6).

The Shannon-Wiener indices (Figure A.7) from samples taken during the baseline monitoring ranged from 1.5 to 4.3. After the heat infiltration, the values decreased to a minimum of 0.8 in the reference well U15 at 10.5 m bgs (7 °C) 27 – 28 days after the infiltration and rose to a maximum of 4.7 in the reference well U15 at 10.5 m bgs (10 °C) 40 - 43 days after the infiltration. At the highest sampled temperatures seven days after the infiltration, 35 °C (well U01, 7.5 m bgs) and 31 °C (well U01, 10.5 m bgs), the calculated Shannon-Wiener indices were 2.1 and 4.2, respectively. The correlation of the Shannon-Wiener indices with the temperatures gave a tau of -0.17 (p-value = 0.11), showing that the alpha diversity and the change in temperature were not significantly correlated. The NMDS (stress = 0.12; Figure 7 and A.8) showed that the microbial communities sampled at different temperatures clustered together, supported by the PERMANOVA that revealed that the communities did not significantly differ between samplings at different temperatures (p-value = 0.45). The PERMANOVA additionally showed that 2% of the variance can be explained by the temperature. The permutation test (Figure A.9) revealed that the dispersion within the microbial communities sampled at different temperatures was statistically significantly different (p-value = 0.001).

The additional t-tests gave p-values of 0.95 and 0.32 (excluding sample 1812_U07_10.5), showing that there was no significant difference in the occurrence of *Thermodesulfovibrionia* between the samples taken before and after the infiltration. The correlation of the QIIME2 level 5 (relative abundances > 5%) results of *Thermodesulfovibrionia* versus the temperatures gave a tau of 0.07 and a p-value of 0.53, revealing that *Thermodesulfovibrionia* did not significantly increase with rising temperature. The correlation of the QIIME2 level 5 results (relative abundances) showed that none of the taxa correlation negatively with a coefficient < -0.4 with

the temperature, while 24 taxa correlated moderately (coefficients of 0.4 – 0.52) and one strongly (coefficient of 0.61) versus the temperature (Figure A.10).

### 3.2 Total cell counts

The total cell numbers are listed in Table A.3 and plotted in Figure 8. Cell numbers in samples taken during the baseline monitoring between October 2018 and April 2019 range from 3.2 * $10^4$ cells/ml to 1.6 * $10^6$ cells/ml. The highest numbers were detected in samples from the downstream well D09 at 7.5 m bgs (3.1 * $10^6$ cells/ml; 13 °C) as well as at 10.5 m bgs (2.0 * $10^6$ cells/ml; 10 °C) taken 27 - 28 days after the infiltration. This temporally coincides with the breakthrough of increased Si concentrations indicating formerly higher elevated temperatures of the sampled water (Figure A.13). In samples taken at the highest temperatures, i. e., 35 °C and 31 °C, seven days after the infiltration, 9.0 * $10^5$ cells/ml (U01 7.5 m bgs) and 7.0 * $10^5$ cells/ml (U01 10.5 m bgs) were determined, respectively. Despite generally rising cell counts with increasing temperatures in the heat effected wells U01 and D09 (Figure A.11), correlation of the total cell counts of all samples with the temperature gave a tau of 0.14 (Figure A.10) and a p-value of 0.18, showing that there is no statistically significant link between the number of cells and the change in temperature.

## 4. Discussion

Utilizing 16S rRNA gene amplicon sequencing and total cell counting, our study showed no statistically significant influence of a heat stress on the composition of the microbial communities and the total number of cells in a shallow aquifer near Wittstock/Dosse, after local groundwater was withdrawn, heated up to 75 °C, and re-infiltrated into the aquifer for about five days. The warmest samples available were the ones taken at moderately increased groundwater temperatures (< 35 °C) from wells that were heated up to ~ 65 °C during the

infiltration, which simulated the thermal effects in the affected space entailed HT-ATES heat storage.

The magnitude of cooling (> 30 °C) indicates that the sampled water was diluted by upstreaming non-heated groundwater. This cooling observed in the aquifer related to mixing of heated water with ground water may represent a typical situation in large areas of an HT-ATES system surrounding the operational space, leading to a moderate temperature rise of the affected groundwater. In summary, the study gives unique insight into the resilience of a groundwater microbiome.

Overall, *Gammaproteobacteria*, *Alphaproteobacteria*, *Bacteroidia*, as well as *Actinobacteria* dominated and *Campylobacteria* (*Thiovulaceae*), *Parcubacteria*, and *Omnitrophicaeota* also occurred frequently. Besides others, *Nitrospira 4-29-1*, *Deltaproteobacteria* (Figures 2 – 5 and A.2 – A.4), and *Dehalococcoidia* were recorded as well in the microbial communities. Whereby, *Dehalococcoidia* correlated positively (coefficient of 0.45) with the temperature (Figure A.10). At 7.5 m, 12.0 m, and 12.7 m depth, *Parcubacteria*, *Gammaproteobacteria*, and *Alphaproteobacteria* were also the three most dominant orders and *Bacteroidia*, *Deltaproteobacteria*, *Actinobacteria*, and *Dehalococcoidia* were recorded as well in an aquifer in the Hainich Critical Zone Exploratory (CZE; Thuringia, Germany) (Yan et al., 2020). Besides others, *Alphaproteobacteria*, *Gammaproteobacteria*, *Deltaproteobacteria*, *Bacteroidia*, *Actinobacteria*, and *Nitrospira* seem to be ubiquitous in groundwater habitats (Beyer et al., 2015; Gülay et al., 2016; Wegner et al., 2019; Yan et al., 2020). In this study, within the *Gammaproteobacteria*, *Pseudomonas* spp (*Pseudomonadaceae*) were the most abundant bacteria. These were present in every sample taken and made up 77.2% of the community in sample 1906-2_U15_10.5 (7 °C) (data not shown). *Pseudomonas* play important roles in soil and aquatic ecosystems and can use a variety of organic compounds as carbon and energy sources. Besides aerobic growth, they can also grow under anaerobic conditions with,

417 e. g., nitrate and even xenobiotic substances as electron acceptors (Madigan et al., 2013).
418 Furthermore, *Pseudomonas* species have been described to degrade TCE (Krumme et al., 1993;
419 Munakata-Marr et al., 1996). Within the *Alphaproteobacteria*, *Novosphingobium* spp
420 (*Sphingomonadaceae*) occurred most frequently as well as *Azambacteria* spp (*Candidatus*)
421 within the *Parcubacteri*a and *Flavobacterium* spp (*Flavobacteriaceae*) within the *Bacteroidia*
422 (data not shown). *Novosphingobium* spp are known to be able to degrade aromatic compounds
423 (Liu et al., 2005), including polycyclic aromatic hydrocarbons (PAHs) (Sohn et al., 2004), and
424 polychlorophenols (Tiirola et al., 2002) and *Flavobacterium* spp can degrade 1,4-dioxane (Sun
425 et al., 2011) as well as pentachlorophenol (PCP) (Crawford & Mohn, 1985; O'Reilly &
426 Crawford, 1989). Furthermore, *Rhodococcus fascians* (*Actinobacteria*, *Nocardiaceae*), which
427 can grow on chlorinated benzoates and polychlorinated biphenyls (PCB) (Abraham et al.,
428 2005), and *Dehalococcoidia* (*Chloroflexi*) that are known for dechlorination of haloorganics
429 (Löffler et al., 2013) were also present, especially at increased temperatures (Figure A.10).
430 Although various bacteria were found that are potentially capable of degrading (chlorinated)
431 contaminants, their presence does not necessarily mean that they perform activities related to
432 the biodegradation of these substances. A contamination with TCE was already reported by
433 Peter et al. (2012), whereby, the former use of the field site as a military airfield led to typical
434 contamination with chlorinated solvents which were used for cleaning. The abundance and
435 diversity of potentially chloroorganics degrading bacteria may indicate that the ecosystem of
436 the microbial community is not negatively affected by the short-term and moderate temperature
437 increase with respect to contaminant degradation. A fast natural attenuation of jet fuel and
438 associated geochemical processes in a tropical aquifer was recently observed (Teramoto et al.,
439 2020), suggesting that elevated temperatures promote microbial processes at mesophilic
440 conditions. Moreover, the artificial enhancements of reductive dechlorination through steam
441 injection in a Danish aquifer (Hunkeler et al., 2011) and ATES (up to 18 °C) in a Dutch aquifer
442 (Sommer et al., 2013) were demonstrated. Thermally enhanced *in situ* bioremediation (ISB; 20

– 30 °C) was successfully applied for chlorinated ethenes in a Czech aquifer, but only with whey as an additional substrate (Němeček et al., 2018). Urban aquifers are often contaminated by hydrocarbons or chloroorganics, and ATES is expected to be preferentially installed in dense populated areas in combination with district heating network. Generally, the concept of combining ATES and microbial degradation in contaminated urban areas is currently discussed and has already been successfully applied (Hunkeler et al., 2011; Sommer et al., 2013; Ni et al., 2015; Němeček et al., 2018 ; Hoekstra et al., 2020). The biodegradation of pollutants can principally be favored at higher temperatures (20 – 30 °C) due to the temperature-dependent increase of microbial metabolic rates (Zeman et al., 2014; Ni et al., 2015; Griebler et al., 2016). Due to our knowledge, there are, however, no field studies investigating the effects of HT-ATES on microbial contaminant degradation.

Besides *Dehalococcoidia*, phylotypes belonging to *Anaerolineae* (*Aminicenantia*), *Micromonosporaceae* (*Actinobacteria*), and *Blastocatellaceae* (*Blastocatellia*), which have been described as being mesophilic (Yamada et al., 2006; Trujillo et al., 2014; Huber et al., 2017), also correlated positively with a coefficient > 0.4 with the temperature (Figure A.10). The rise of the groundwater temperature into a mesophilic range, might have stimulated their growth and activity (Griebler et al., 2016). While these families made up < 5% of the microbial communities, the order *Thermodesulfovibrionia* occurred more frequently. This order, containing thermophilic members, was present in samples from the baseline monitoring, here, with the highest percentage of 8.4% in sample 1812_U07_10.5, and in samples after the infiltration (Figure A.3). As expectable due to the short duration of temperatures in the thermophilic range, t-tests showed that there was no significant difference in the occurrence of *Thermodesulfovibrionia* between the baseline samples and the post-infiltration samples (p-value = 0.95), even when the sample 1812_U07_10.5 was excluded from the analysis (p-value = 0.32). The correlation versus the temperature additionally revealed that the abundance did not significantly increase with rising temperature (tau = 0.07 and p-value = 0.53).

469 *Thermodesulfovibrionia* outcompeted other microorganisms in a thermophilic (55 °C)
470 anaerobic digestion reactor (Yamada et al., 2019). This class could have also been more
471 dominant during the field experiment at higher groundwater temperatures, but this might have
472 remained unnoticed due to the lack of samples at temperatures ≥ 35 °C. However, the detection
473 of *Thermodesulfovibrionia* in the investigated aquifer in general seems to be no exception
474 because the class was also recorded in groundwater samples taken between 5.1 and 88 m depth
475 in a near-surface aquifer in the Hainich CZE. There, the average occurrence in the microbial
476 community was 7.0 ± 7.9% and the highest relative abundances (21.2 ± 6.5%) were detected in
477 samples from a depth of 50 m, with groundwater temperatures of 9.47 ± 0.04 °C (Yan et al.,
478 2020).

479 The alpha diversity fluctuated in the samples, even in those from the baseline monitoring
480 (Figure A.7), but no significant correlation between the calculated Shannon-Wiener indices and
481 the change in temperature was determined (tau = -0.17, p-value = 0.11). Moreover, the NMDS
482 (Figures 7 and A.8) and the PERMANOVA showed that there was no statistically significant
483 difference between the microbial communities at different temperatures. The high dispersion
484 within the samples at low (reference) temperatures, as revealed by the permutation test (Figure
485 A.9), and/or the low number of samples at elevated temperatures (12 – 35 °C), could cover up
486 possible effects. Seasonal variations in the microbial communities, as shown by other studies
487 (Waldrop & Firestone, 2006; Wilhartitz et al., 2009; Zhou et al., 2012), could contribute to the
488 high dispersion, distorting the data even further. Contrary to this study, Brielmann et al. (2009)
489 showed a weak significant positive correlation between bacterial diversity (Shannon-Wiener
490 diversity inferred from T-RFLP fingerprints) and temperature in groundwater samples from an
491 oligotrophic shallow aquifer impacted by a heat plume (≤ 21 °C) from a facility's discharge,
492 where the temperature explained 5% of the variation in the samples. Although the temperature
493 exposure was higher in our experiment, only Friedman tests and pairwise comparisons with

494 Wilcoxon signed-rank tests revealed individual statistically significant differences between
495 microbial communities from specific samplings in heat affected and unaffected wells. Overall,
496 no significant effects on the microbial communities could be detected. This could be explained
497 by the short and discontinuous heat exposure as well as the fast cooling that occurred in the
498 aquifer, including recovery through the inflow of new groundwater. Beyond that, it is important
499 to note that sediments carry the majority of the microbial biomass, especially in oligotrophic
500 aquifers (Alfreider et al., 1997; Griebler et al., 2002; Wilhartitz et al., 2009; Flynn et al., 2013),
501 and significant changes in the microbial diversity could occur at a moderate (and chronic)
502 temperature increase (Zogg et al., 1997; Bradford et al., 2008; Yergeau et al., 2012) or at high
503 (≥ 45 °C) temperatures (Bonte et al., 2013a). Recently, we studied biodiversity changes due to
504 temperature (12, 25, 37, 45, 60, and 80 °C) in aerobic sediment/groundwater laboratory
505 microcosms using material from the aquifer in Wittstock/Dosse incubated for up to 49 days. At
506 12, 25, and 37 °C, the microbial communities did not change significantly, while the ones
507 incubated at 45 and 60 °C showed significant changes and differed from each other and the
508 others (Metze et al., 2020). Bonte et al. (2013a) also detected a bacterial community shift
509 (especially in sediments) to a community dominated by thermophilic fermenters and sulfate
510 reducers at temperatures > 45 °C in laboratory experiments using sediment and groundwater of
511 two Dutch anoxic aquifers and incubation temperatures between 5 – 80 °C.

512 The total cell counts from samples taken during the baseline monitoring ranged from $3.2 * 10^4$
513 - $1.6 * 10^6$ cells $ml^{-1}$ (Table A.3, Figure 8). These values reflect the range expected for pristine
514 groundwater, i. e., $10^4$ to $10^6$ cells $ml^{-1}$ (Goldscheider et al., 2006). After the heat stress, the
515 values rose to a maximum of $3.1 * 10^6$ cells $ml^{-1}$ in the downstream well D09 at 7.5 m bgs (13
516 °C) 27 – 28 days after the infiltration, which is still within the normal range. This temporally
517 coincides with increased Si concentrations (Figure A.13), which might show the release of
518 nutrients (P and Fe) from silicate minerals that stimulate microbial growth (Roberts Rogers &

519 Bennett, 2004). At the highest sampled temperatures seven days after the infiltration, 35 °C (9
520 * $10^5$ cells/ml) and 31 °C (7 * $10^5$ cells/ml), neither a pronounced decrease nor an increase of
521 cell numbers was detected. When the total cell counts were viewed for the heat impacted wells
522 individually, they revealed (very) strong and moderate positive correlations versus the
523 temperatures (Figure A.11). However, no statistically significant link between the number of
524 cells and the change in temperature was detected overall (tau = 0.14, p-value = 0.18). This is in
525 accordance with the results from Brielmann et al. (2009), where no significant differences of
526 the total bacterial cell counts in groundwater samples from heat-impacted (8.5 – 17.8 °C) and
527 non-impacted (11 ± 1 °C) areas was detected (Brielmann et al., 2009). However, when the total
528 cell counts were viewed for the heat-impacted wells individually, they correlated with
529 temperatures.

530 In summary, the temporally limited heat stress in our experiment did not significantly change
531 the microbial communities and the total number of cells in groundwater; therefore, our results
532 may indicate a functional resilience of the heterotrophic aquifer ecosystem (assuming that cells
533 were not inactivated during contact with the hot water), whereby, the high biodiversity (Griebler
534 & Avramov, 2015) could contribute to attenuate the effects of the heating. On the contrary,
535 divers microbial communities were also reported in geothermally used aquifers (Lerm et al.,
536 2011). In deep (~1.300 m bgs) saline aquifers (54 °C) affected by the operation of geothermal
537 plants, the composition of microbial communities as well as the quantities of cells and genes
538 differed in fluids collected from the cold (45 – 54 °C) and the warm (80 – 87 °C) wells, with
539 higher bacterial abundances at lower temperatures (Lerm et al., 2013; Westphal et al., 2016).
540 Notably, groundwater fauna - unicellular organisms, specifically, protists like ciliates,
541 flagellates, and amoebae, as well as multicellular animals, e. g., crustaceans, snails, and worms
542 (Schmidt & Hahn, 2012) - is more sensitive to temperature changes (Colson-Proch et al., 2010;
543 Brielmann et al., 2011; Foulquier et al., 2011; Griebler et al., 2016) and might have been

affected in the course of our field experiment, but investigating such effects was beyond the scope of this study.

## Conclusion

In this study, the temporally limited heat stress induced in a shallow aquifer near Wittstock/Dosse did not lead to significant shifts in the groundwater microbiome. The results indicate that the microflora was resilient to the short-term thermal stress; potential losses of microbial functions could not be detected by the applied methods. However, correlation coefficient > 0.4 (Relative abundances versus temperature) of some taxa hint towards expectable stronger effects at longer sustained higher temperatures. Similarly, the same can be inferred from the total cell counts where (very) strong and moderate positive correlations with increasing temperatures in individual heat effected wells were concealed by the large natural variability when all samplings are considered.

In total, the results of this study support earlier findings which recently showed that low temperature (LT)-ATES is generally not extensively disadvantageous for a groundwater microbiome. Correspondingly, our results indicate that the aquifer microbiome of an affected space of a HT-ATES system, which is exposed to temperatures comparable to the operational space of a LT-ATES system, will not be considerably affected. However, the investigated heat impact in this study, does not allow to derive recommendation for long term-predictions of microbial community responses during the full operation of a HT-ATES system (> 60 °C), considering both the operational space and the affected space. Therefore, future studies will address higher temperatures, longer heat exposures, and cyclical heat impacts to close this gap in knowledge regarding expectable effects on microbial communities for evaluating environmental impacts of HT-ATES systems.

## Acknowledgements

We would like to thank Marco Mahnecke, Nilufar Zarrabi, Florian Tschernikl, and Stephan Krantz for help with the field or/and lab work. Additional thanks to Katja Nerlich and Nicole Steinbach for the introduction to the DAPI-cell counting procedures and the Illumina MiSeq amplicon sequencing procedures, respectively.

## Funding

This work was part of the TestUM-Aquifer project (grant number 03G0875B) which belongs to the Verbundprojekt "Forschung für Nachhaltige Entwicklung (FONA3)" funded by the Bundesministerium für Bildung und Forschung (BMBF).

## Author's statement

We, the authors, declare no competing interests.

## References

Abraham W-R, Wenderoth D F, & Gläßer W (2005) Diversity of biphenyl degraders in a chlorobenzene polluted aquifer. *Chemosphere 58*, 529 – 533.

Alfreider A, Krössbacher M, & Psenner R (1997) Groundwater samples do not reflect bacterial densities and activity in subsurface systems. *Water Research 31 (4)*, 832 – 840.

Anderson M J (2001) A new method for non- parametric multivariate analysis of variance. *Austral Ecology 26*, 32 – 46.

Anderson M J & Walsh D C I (2013) PERMANOVA, ANOSIM, and the Mantel test in the face of heterogeneous dispersions: what null hypothesis are you testing? *Ecological monographs 83*, 557 – 74.

588 Arning E, Kölling M, Schulz H D, Panteleit B, & Reichling J (2006) Einfluss oberflächennaher
589 Wärmegewinnung auf geochemische Prozesse im Grundwasserleiter. *Grundwasser 11*, 27 –
590 39.

591 Beyer A, Rzanny M, Weist A, Möller S, Burow K, Gutmann F, Neumann S, Lindner J, Müsse
592 S, Brangsch H, Stoiber-Lipp J, Lonschinski M, Merten D, Büchel G, & Kothe E (2015) Aquifer
593 community structure in dependence of lithostratigraphy in groundwater reservoirs.
594 *Environmental Science and Pollution Research 22*, 19342 – 19351.

595 Bolyen E, Rideout J R, Dillon M R, et al. (2019) Reproducible, interactive, scalable and
596 extensible microbiome data science using QIIME 2. *Nature Biotechnology 37*, 852 – 857.

597 Bonte M, Röling W F M, Zaura E, van der Wielen P W J J, Stuyfzand P J, & van Breukelen B
598 M (2013a) Impacts of Shallow Geothermal Energy Production on Redox Processes and
599 Microbial Communities. *Environmental Science & Technology 47*, 14476 − 14484.

600 Bonte M, Stuyfzand P J, van den Berg G A, & Hijnen W A M (2011) Effects of aquifer thermal
601 energy storage on groundwater quality and the consequences for drinking water production: a
602 case study from the Netherlands. *Water Science & Technology 63.9*, 1922 – 1931.

603 Bonte M, van Breukelen B M, & Stuyfzand P J (2013b) Temperature-induced impacts on
604 groundwater quality and arsenic mobility in anoxic aquifer sediments used for both drinking
605 water and shallow geothermal energy production. *Water Research 47*, 5088 – 5100.

606 Bradford M A, Davies C A, Frey S D, Maddox T R, Melillo J M, Mohan J E, Reynolds J F,
607 Treseder K K, & Wallenstein M D (2008) Thermal adaptation of soil microbial respiration to
608 elevated temperature. *Ecology Letters 11*, 1316 – 1327.

609 Brielmann H, Griebler C, Schmidt S I, Michel R, & Lueders T (2009) Effects of thermal energy
610 discharge on shallow groundwater ecosystems. *FEMS Microbiology Ecology 68*, 273 – 286.

611 Brielmann H, Lueders T, Schreglmann K, Ferraro F, Avramov M, Hammerl V, Blum P, Bayer
612 P, & Griebler C (2011) Oberflächennahe Geothermie und ihre potenziellen Auswirkungen auf
613 Grundwasserökosysteme. *Grundwasser 16*, 77 - 91.

614 Brons H E, Griffioen J, Appelo C A J, & Zehnder A J B (1991) (Bio)geochemical reactions in
615 aquifer material from a thermal energy storage site. *Water Research 25*, 729 – 736.

616 Callahan B J, McMurdie P J, Rosen M J, Han A W, Johnson A J A, & Holmes S P (2016a)
617 DADA2: High-resolution sample inference from Illumina amplicon data. *Nature Methods 13*,
618 581 – 583.

619 Callahan B J, Sankaran K, Fukuyama J A, McMurdie P J, & Holmes S P (2016b) Bioconductor
620 Workflow for Microbiome Data Analysis: from raw reads to community analyses.
621 *F1000Research 5:1492*.

622 Christ M J & David M B (1996) Temperature and moisture effects on the production of
623 dissolved organic carbon in a Spodosol. *Soil Biology and Biochemistry 28*, 1191 – 1199.

624 Colson-Proch C, Morales A, Hervant F, Konecny L, Moulin C, & Douady CJ (2010) First
625 cellular approach of the effects of global warming on groundwater organisms: a study of the
626 HSP70 gene expression. *Cell Stress Chaperones 15*, 259 – 270.

627 Crawford R L & Mohn W W (1985) Microbiological removal of pentachlorophenol from soil
628 using a *Flavobacterium*. *Enzyme and Microbial Technology 7*, 617 – 620.

629 Dahmke A, Schwanebeck M, Dethlefsen F, Beyer C, Delfs J-O, Wang B, Schäfer D, Köber R,
630 Bauer S, Menberg K, Tissen C, & Koch F (2020) Räumliches Ausbaupotenzial zur Nutzung
631 des geologischen Untergrunds zur Wärmeversorgung. Oral presentation at DER
632 GEOTHERMIEKONGRESS 2020, Workshop 4 – Umweltwirkungen und umweltverträglicher
633 Ausbau der oberflächennahen Geothermie, 09.11.2020, virtual conference

Degenhart H, Holstenkamp L, Kohrs A K, Neidig P, Opel O, Schomerus T, Strodel N, Michalzik D, Steffahn J, Porcello K, Meisel M, Weber J, Schönebeck J, & Kruck O (2019) Aquifer Thermal Energy Storage (ATES): Developing Areas of Application for Medium-Deep ATES Systems in Northern Germany under Economic/Financial, Geological/Technical, Environmental Chemistry and Legal/Support Policy Aspects. Final report, Leuphana University of Lüneburg, Lüneburg, Germany.

Drijver B, van Aarssen M, & de Zwart B (2012) High-temperature aquifer thermal energy storage (HT-ATES): sustainable and multi-usable. Proceedings at The 12th International Conference on Energy Storage, Innostock 2012.

Faith D P, Minchin P R & Belbin L (1987) Compositional dissimilarity as a robust measure of ecological distance. *Vegetatio 69*, 57 – 68.

Fleuchaus P, Godschalk B, Stober I, & Blum P (2018) Worldwide application of aquifer thermal energy storage – A review. *Renewable and Sustainable Energy Reviews 94*, 861 – 876.

Flynn T M, Sanford R A, Ryu H, Bethke C M, Levine A D, Ashbolt N J, & Santo Domingo J W (2013) Functional microbial diversity explains groundwater chemistry in a pristine aquifer. *BMC Microbiology 13:146*.

Foulquier A, Malard F, Mermillod-Blondin F, Montuelle B, Doledec S, Volat B, & Gibert J (2011) Surface water linkages regulate trophic interactions in a groundwater food web. *Ecosystems 14*, 1339 – 1353.

Fox J & Weisberg S (2019) An {R} Companion to Applied Regression, Third Edition. Sage, Thousand Oaks, CA, USA.

Goldscheider N, Hunkeler D, & Rossi P (2006) Review: Microbial biocenoses in pristine aquifers and an assessment of investigative methods. *Hydrogeology Journal 0*, 1 - 16.

Griebler C & Avramov M (2015) Groundwater ecosystem services: a review. *Groundwater–Surface-Water Interactions 34*, 355 – 367.

Griebler C, Brielmann H, Haberer C M, Kaschuba S, Kellermann C, Stumpp C, Hegler F, Kuntz D, Walker-Hertkorn S, & Lueders T (2016) Potential impacts of geothermal energy use and storage of heat on groundwater quality, biodiversity, and ecosystem processes. *Environmental Earth Sciences 75:1391*.

Griebler C, Mindl B, Slezak D, & Geiger-Kaiser M (2002) Distribution patterns of attached and suspended bacteria in pristine and contaminated shallow aquifers studied with an in situ sediment exposure microcosm. *Aquatic Microbial Ecology 28*, 117 – 129.

Griffioen J & Appelo C A J (1993) Nature and extent of carbonate precipitation during aquifer thermal energy storage. *Applied Geochemistry 8*, 161 - 176.

Gülay A, Musovic S, Albrechtsen H-J, Abu Al-Soud W, Sørensen S J, & Smets B F (2016) Ecological patterns, diversity and core taxa of microbial communities in groundwater-fed rapid gravity filters. *The ISME Journal 10*, 2209 – 2222.

Hähnlein S, Blum P, & Bayer P (2011) Oberflächennahe Geothermie – aktuelle rechtliche Situation in Deutschland. *Grundwasser – Zeitschrift der Fachsektion Hydrogeologie 16*, 69 – 75.

Hoekstra N, Pellegrini M, Bloemendal M, Spaak G, Andreu Gallego A, Rodriguez Comins J, Grotenhuis T, Picone S, Murrell A J, Steeman H J, Verrone A, Doornenbal P, Christophersen M, Bennedsen L, Henssen M, Moinier S, & Saccani C (2020) Increasing market opportunities for renewable energy technologies with innovations in aquifer thermal energy storage. *Science of the Total Environment 709*, 136142.

679 Holm T R, Eisenreich S J, Rosenberg H L, & Holm N P (1987) Groundwater geochemistry of
680 short-term aquifer thermal energy storage test cycles. *Water Resources Research 23*, 1005 -
681 1019.

682 Hornbruch G et al. TestUM: A test site for controlled field experiments in a shallow aquifer
683 within the scope of the energy transition research - experimental design and database. In
684 preparation.

685 Huber K J, Pascual J, Foesel B U, & Overmann J (2017) Blastocatellaceae. In: *Bergey's Manual*
686 *of Systematics of Archaea and Bacteria (BMSAB)*, Bergey's Manual Trust 2017.

687 Hunkeler D, Abe Y, Broholm M M, Jeannottat S, Westergaard C, Suhr Jacobsen C, Aravena
688 R, & Bjerg P L (2011) Assessing chlorinated ethene degradation in a large scale contaminant
689 plume by dual carbon–chlorine isotope analysis and quantitative PCR. *Journal of Contaminant*
690 *Hydrology 119*, 69 - 79.

691 Jenne E A, Andersson O, & Willemsen A (1992) Well, hydrology, and geochemistry problems
692 encountered in ATES systems and their solutions. In: Jenne E A (Ed.) Aquifer Thermal Energy
693 (Heat and Chill) Storage: Proceedings of the 27th Intersociety Energy Conversion Engineering
694 Conference. San Diego, CA.

695 Jesußek A, Grandel S, & Dahmke A (2013a) Impacts of subsurface heat storage on aquifer
696 hydrogeochemistry. *Environmental Earth Sciences 69*: 1999 – 2012.

697 Jesußek A, Koeber R, Grandel S, & Dahmke A (2013b) Aquifer heat storage: sulfate reduction
698 with acetate at increased temperatures. *Environmental Earth Sciences 69*: 1763 – 1771.

699 Kaiser K, Kaupenjohann M, & Zech W (2001) Sorption of dissolved organic carbon in soils:
700 effects of soil sample storage, soil-to-solution ratio, and temperature. *Geoderma 99*, 317 – 328.

Kassambara A (2020a) ggpubr: 'ggplot2' Based Publication Ready Plots. R package version 0.4.0. https://CRAN.R-project.org/package=ggpubr.

Kassambara A (2020b) rstatix: Pipe-Friendly Framework for Basic Statistical Tests. R package version 0.6.0. https://CRAN.R-project.org/package=rstatix.

Klindworth A, Pruesse E, Schweer T, Peplies J, Quast C, Horn M, & Glöckner F O (2013) Evaluation of general 16S ribosomal RNA gene PCR primers for classical and next-generation sequencing-based diversity studies. *Nucleic Acids Research 41 (1)*, 1 – 11.

Krumme M L, Timmis K N, & Dwyer D F (1993) Degradation of Trichloroethylene by Pseudomonas cepacia G4 and the Constitutive Mutant Strain G4 5223 PR1 in Aquifer Microcosms. *Applied and Environmental Microbiology 59 (8)*, 2746 – 2749.

Kruskal J B (1964a) Multidimensional scaling by optimizing goodness-of-fit to a nonmetric hypothesis. *Psychometrika 29*, 1 – 28.

Kruskal J B (1964b) Nonmetric multidimensional scaling: a numerical method. *Psychometrika 29*, 115 – 129.

Lee K S (2010) A Review on Concepts, Applications, and Models of Aquifer Thermal Energy Storage Systems. *Energies 3 (6)*, 1320 – 1334.

Lerm S, Alawi M, Miethling-Graff R, Seibt A, Wolfgramm M, Rauppach K, & Würdemann H (2011) Mikrobiologisches Monitoring in zwei geothermisch genutzten Aquiferen Norddeutschlands. *Zeitschrift geologischer Wissenschaften* 39 (4), 195 - 212.

Lerm S, Westphal A, Miethling-Graff R, Alawi M, Seibt A, Wolfgramm M, & Würdemann H (2013) Thermal effects on microbial composition and microbiologically induced corrosion and

722 mineral precipitation affecting operation of a geothermal plant in a deep saline aquifer.
723 *Extremophiles 17 (2)*, 311–327.

724 Liu Z-P, Wang B-J, Liu Y-H, & Liu S-J (2005) *Novosphingobium taihuense* sp. nov., a novel
725 aromatic-compound-degrading bacterium isolated from Taihu Lake, China. *International*
726 *Journal of Systematic and Evolutionary Microbiology 55*, 1229 – 1232.

727 Löffler F E, Yan J, Ritalahti K M, Adrian L, Edwards E A, Konstantinidis K T, Müller J A,
728 Fullerton H, Zinder S H, & Spormann A M (2013) *Dehalococcoides mccartyi* gen. nov., sp.
729 nov., obligately organohalide-respiring anaerobic bacteria relevant to halogen cycling and
730 bioremediation, belong to a novel bacterial class, *Dehalococcoidia* classis nov., order
731 *Dehalococcoidales* ord. nov. and family *Dehalococcoidaceae* fam. nov., within the phylum
732 *Chloroflexi*. *International Journal of Systematic and Evolutionary Microbiology 63*, 625 – 635.

733 Lüders K, Dahmke A, Fiedler M, & Köber R (2020) Temperature influence on mobilisation
734 and (re)fixation of trace elements and heavy metals in column tests with aquifer sediments from
735 10 to 70 °C. *Water Research 169:115266*.

736 Lüders K, Firmbach L, Ebert M, Dahmke A, Dietrich P, & Köber R (2016) Gas-phase formation
737 during thermal energy storage in near-surface aquifers - experimental and modelling results.
738 *Environmental Earth Sciences 75, 1404*.

739 Madigan M T, Martinko J M, Stahl D A, & Clark D P (2013) Brock Mikrobiologie Pearson
740 Deutschland GmbH, Hallbergmoos, Germany.

741 Martin M (2011) Cutadapt removes adapter sequences from high-throughput sequencing reads.
742 *EMBnet.journal 17.1*, 10 - 12.

743 Metze D, Popp D, Schwab L, Keller N-S, Nunes da Rocha U, Richnow H, & Vogt C (2020)
744 Temperature management potentially affects carbon mineralization capacity and microbial
745 community composition of a shallow aquifer. *FEMS Microbiology Ecology*, fiaa261.

746 Minchin P R (1987) An evaluation of relative robustness of techniques for ecological
747 ordinations. *Vegetatio 69*, 89 – 107.

748 Munakata-Marr J, McCarty P L, Shields M S, Reagin M, & Francesconi S C (1996)
749 Enhancement of Trichloroethylene Degradation in Aquifer Microcosms Bioaugmented with
750 Wild Type and Genetically Altered Burkholderia (Pseudomonas) cepacia G4 and PR1.
751 *Environmental Science & Technology 30*, 2045 – 2052.

752 Němeček J, Steinová J, Špánek R, Pluhař T, Pokorný P, Najmanová P, Knytl V, & Černík M
753 (2018) Thermally enhanced in situ bioremediation of groundwater contaminated with
754 chlorinated solvents – A field test. *Science of the Total Environment 622 – 623*, 743 – 755.

755 Ni Z, van Gaans P, Smit M, Rijnaarts H, & Grotenhuis T (2015) Biodegradation of *cis*-1,2-
756 Dichloroethene in Simulated Underground Thermal Energy Storage Systems. *Environmental*
757 *Science & Technology 49*, 13519 – 13527.

758 Novo A V, Bayon J R, Castro-Fresno D, & Rodriguez-Hernandez J (2010) Review of seasonal
759 heat storage in large basins: Water tanks and gravel-water pits. *Applied Energy 87 (2)*, 390 -
760 397.

761 Oksanen J, Guillaume Blanchet F, Friendly M, Kindt R, Legendre P, McGlinn D, Minchin P
762 R, O'Hara R B, Simpson G L, Solymos P, Stevens M H H, Szoecs E, & Wagner H (2020)
763 vegan: Community Ecology Package. R package version 2.5-7. https://CRAN.R-
764 project.org/package=vegan.

765 O'Reilly K T & Crawford R L (1989) Degradation of Pentachlorophenol by Polyurethane-
766 Immobilized *Flavobacterium* Cells. *Applied and Environmental Microbiology 55 (9),* 2113 –
767 2118.

768 Palmer C D & Cherry J A (1984) Geochemical reactions associated with low-temperature
769 thermal energy storage in aquifers. *Canadian Geotechnical Journal 21,* 475 – 488.

770 Pedersen T L (2020) patchwork: The Composer of Plots. R package version 1.1.0.
771 https://CRAN.R-project.org/package=patchwork.

772 Peter A, Hornbruch G, & Dahmke A (2011) $CO_2$ leakage test in a shallow aquifer for
773 investigating the geochemical impact of $CO_2$ on groundwater and for developing monitoring
774 methods and concepts. *Energy Procedia 4,* 4148 – 4153.

775 Peter A, Lamert H, Beyer M, Hornbruch G, Heinrich B, Schulz A, Geistlinger H, Schreiber B,
776 Dietrich P, Werban U, Vogt C, Richnow H.-H., Großmann J, & Dahmke A (2012) Investigation
777 of the geochemical impact of $CO_2$ on shallow groundwater: design and implementation of a
778 $CO_2$ injection test in Northeast Germany. *Environmental Earth Sciences 67,* 335 – 349.

779 R Core Team (2020) R: A language and environment for statistical computing. R Foundation
780 for Statistical Computing, Vienna, Austria. URL https://www.R-project.org/.

781 Reineke W & Schlömann M (2015) Umweltmikrobiologie. Springer-Verlag, Berlin
782 Heidelberg.

783 Roberts Rogers J & Bennett P C (2004) Mineral stimulation of subsurface microorganisms:
784 release of limiting nutrients from silicates. *Chemical Geology 203,* 91 – 108.

785 Rudis B (2020) hrbrthemes: Additional Themes, Theme Components and Utilities for 'ggplot2'.
786 R package version 0.8.0. https://CRAN.R-project.org/package=hrbrthemes.

RStudio Team (2020) RStudio: Integrated Development for R. RStudio, PBC, Boston, MA URL http://www.rstudio.com/.Schmidt S I & Hahn H J (2012) What is groundwater and what does this mean to fauna? – An opinion. *Limnologica 42,* 1 – 6.

Schmidt S I & Hahn H J (2012) What is groundwater and what does this mean to fauna? – An opinion. Limnologica 42, 1 – 6.

Sohn J H, Kwon K K, Kang J-H, Jung H-B, & Kim S-J (2004) *Novosphingobium pentaromativorans* sp. nov., a high-molecular-mass polycyclic aromatic hydrocarbon-degrading bacterium isolated from estuarine sediment. *International Journal of Systematic and Evolutionary Microbiology 54,* 1483 – 1487.

Sommer W, Drijver B, Verburg R, Slenders H, de Vries E, Dinkla I, Leusbrock I, & Grotenhuis T (2013) Combining shallow geothermal energy and groundwater remediation. European Geothermal Congress 2013, Pisa, Italy, 3 - 7 June 2013.

Sommer W, Valstar J, Leusbrock I, Grotenhuis T, & Rijnaarts H (2015) Optimization and spatial pattern of large-scale aquifer thermal energy storage. *Applied Energy 137,* 322 – 337.

Sun B, Ko K, & Ramsay J A (2011) Biodegradation of 1,4-dioxane by a *Flavobacterium. Biodegradation 22,* 651 – 659.

Teramoto E H, Vogt C, Martins Baessa M P, Polese L, Soriano A U, Chang H K, & Richnow H H (2020) Dynamics of hydrocarbon mineralization characterized by isotopic analysis at a jet-fuel-contaminated site in subtropical climate. *Journal of Contaminant Hydrology 234:103684*.

Tiirola M A, Männistö M K, Puhakka J A, & Kulomaa M S (2002) Isolation and Characterization of *Novosphingobium* sp. Strain MT1, a Dominant Polychlorophenol-Degrading Strain in a Groundwater Bioremediation System. *Applied and Environmental Microbiology 68 (1),* 173 – 180.

Trujillo M E, Hong K, & Genilloud O (2014) The Family *Micromonosporaceae*. In: Rosenberg E, DeLong E F, Lory S, Stackebrandt E, & Thompson F (eds) The Prokaryotes. Springer, Berlin, Heidelberg.

Waldrop M P & Firestone M K (2006) Seasonal Dynamics of Microbial Community Composition and Function in Oak Canopy and Open Grassland Soils. *Microbial Ecology 52,* 470 – 479.

Wegner C-E, Gaspar M, Geesink P, Herrmann M, Marz M, & Küsel K (2019) Biogeochemical Regimes in Shallow Aquifers Reflect the Metabolic Coupling of the Elements Nitrogen, Sulfur, and Carbon. *Applied and Environmental Microbiology 85 (5),* e02346-18.

Westphal A, Lerm S, Miethling-Graff R, Seibt A, Wolfgramm M, & Würdemann H (2016) Effects of plant downtime on the microbial community composition in the highly saline brine of a geothermal plant in the north German basin. *Applied Microbiology and Biotechnology 100,* 3277 – 3290.

Wickham H (2007) Reshaping Data with the reshape Package. *Journal of Statistical Software 21 (12),* 1 – 20.

Wickham H (2016) ggplot2: Elegant Graphics for Data Analysis. Springer-Verlag, New York.

Wickham H, Averick M, Bryan J, Chang W, D'Agostino McGowan L, François R, Grolemund G, Hayes A, Henry L, Hester J, Kuhn M, Pedersen T L, Miller E, Bache S M, Müller K, Ooms J, Robinson D, Seidel D P, Spinu V, Takahashi K, Vaughan D, Wilke C, Woo K, & Yutani H (2019) Welcome to the tidyverse. *Journal of Open Source Software 4 (43),* 1686.

Wickham H, François R, Henry L, & Müller K (2020) dplyr: A Grammar of Data Manipulation. R package version 1.0.2. https://CRAN.R-project.org/package=dplyr.

832 Wilhartitz I C, Kirschner A K T, Stadler H, Herndl G J, Dietzel M, Latal C, Mach R L, &
833 Farnleitner A H (2009) Heterotrophic prokaryotic production in ultraoligotrophic alpine karst
834 aquifers and ecological implications. *FEMS Microbiology Ecology 68*, 287 – 299.

835 Yamada T, Hamada M, Kurobe M, Harada J, Giri S, Tsuji H, & Daimon H (2019) Prokaryotic
836 Community Structures in a Thermophilic Anaerobic Digestion Reactor Converting Poly(L-
837 Lactic Acid) for a Long Period Revealed by 16S rRNA Gene Amplicon Sequencing.
838 *Microbiology Resource Announcements 8 (29)*, 8:e00679-19.

839 Yamada T, Sekiguchi Y, Hanada S, Imachi H, Ohashi A, Harada H, & Kamagata Y (2006)
840 *Anaerolinea thermolimosa* sp. nov., *Levilinea saccharolytica* gen. nov., sp. nov. and *Leptolinea*
841 *tardivitalis* gen. nov., sp. nov., novel filamentous anaerobes, and description of the new classes
842 *Anaerolineae* classis nov. and *Caldilineae* classis nov. in the bacterial phylum *Chloroflexi*.
843 *International Journal of Systematic and Evolutionary Microbiology 56 (6)*, 1331 – 1340.

844 Yan L, Herrmann M, Kampe B, Lehmann R, Totsche K U, & Küsel K (2020) Environmental
845 selection shapes the formation of near-surface groundwater microbiomes. *Water Research 170*,
846 115341.

847 Yergeau E, Bokhorst S, Kang S, Zhou J, Greer C W, Aerts R, & Kowalchuk G A (2012) Shifts
848 in soil microorganisms in response to warming are consistent across a range of Antarctic
849 environments. *The ISME Journal 6*, 692 – 702.

850 Zeman N R, Renno M I, Olson M R, Wilson L P, Sale T C, & De Long S K (2014) Temperature
851 impacts on anaerobic biotransformation of LNAPL and concurrent shifts in microbial
852 community structure. *Biodegradation 25*, 569 – 585.

853 Zhou Y, Kellermann C, & Griebler C (2012) Spatio-temporal patterns of microbial
854 communities in a hydrologically dynamic pristine aquifer. *FEMS Microbiology Ecology 81*,
855 230 – 242.

856 Zogg G P, Zak D R, Ringelberg D B, MacDonald N W, Pregitzer K S, & White D C (1997)
857 Compositional and Functional Shifts in Microbial Communities Due to Soil Warming. *Soil*
858 *Science Society of America Journal 61*, 475 – 481.

**Figure 1 (Keller et al.)**

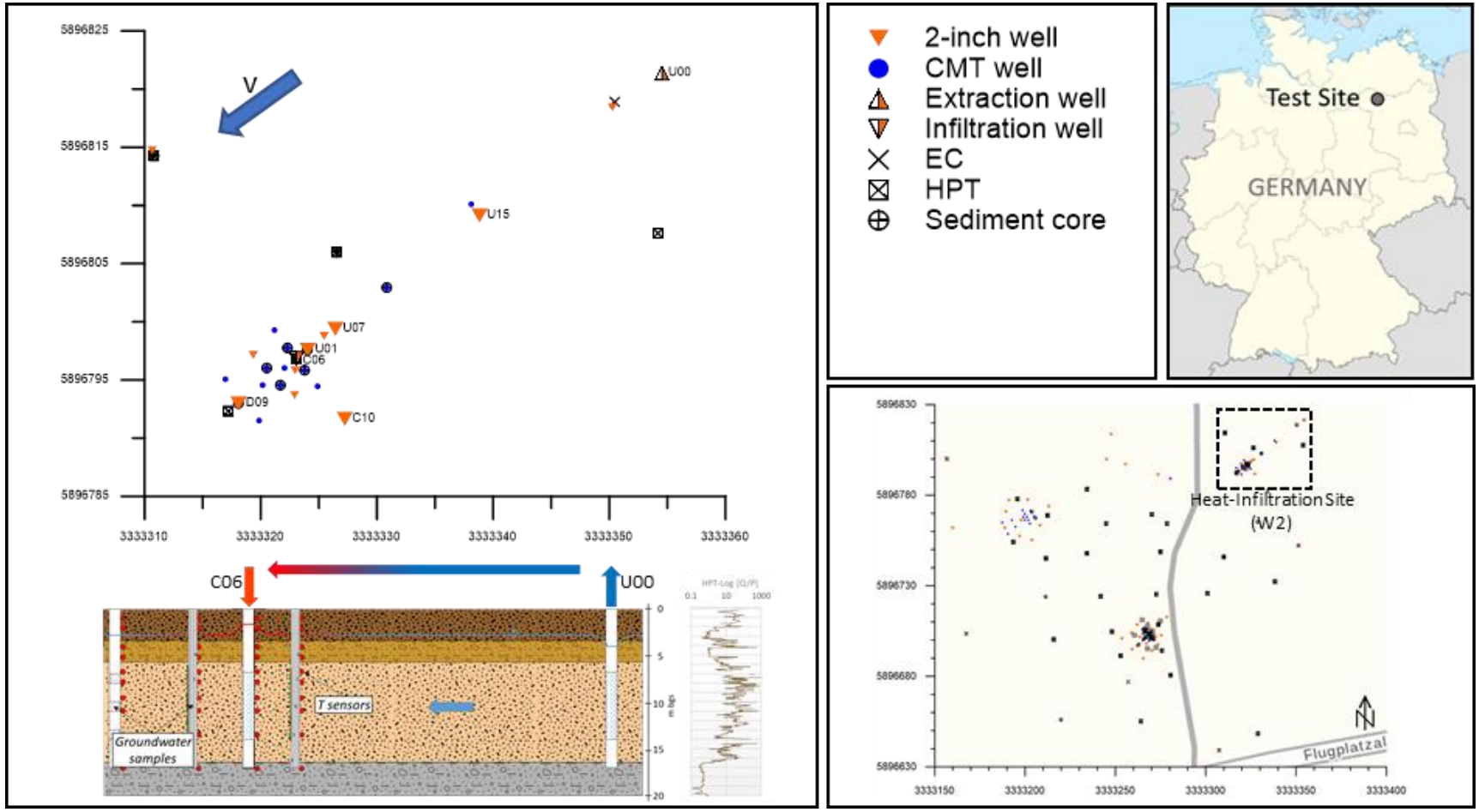


**Figure 1:** Overview of the whole test site area (right) and map of the monitoring network for the heat infiltration test (left). The 2" extraction well (U00; upturned white-orange triangle) is located 40 m upstream of the 2" infiltration well (C06; downturned white-orange triangle). The five 2" sampling wells (bigger orange triangles) have filter stretches from 7 – 8, 10 – 11, and 13 – 14 m below ground surface (bgs) and the 12 multilevel (ML) sampling wells (blue dots) have 10 cm filtered sections at 5, 7.5, 10.5, 13.5 m, and 16.5 m bgs. The groundwater flows in West-South-West direction. The groundwater was extracted from the well 40 m upstream over a filter stretch from 7 – 14 m bgs, pumped into an argon covered buffer tank, then, through a heat exchanger, where it was heated to 75 ° C, and further through a second buffer tank where it degassed. From there, the water was gravitationally infiltrated into the nearby infiltration well over a filter stretch from 7 – 14 m bgs.

**Figure 2 (Keller et al.)**

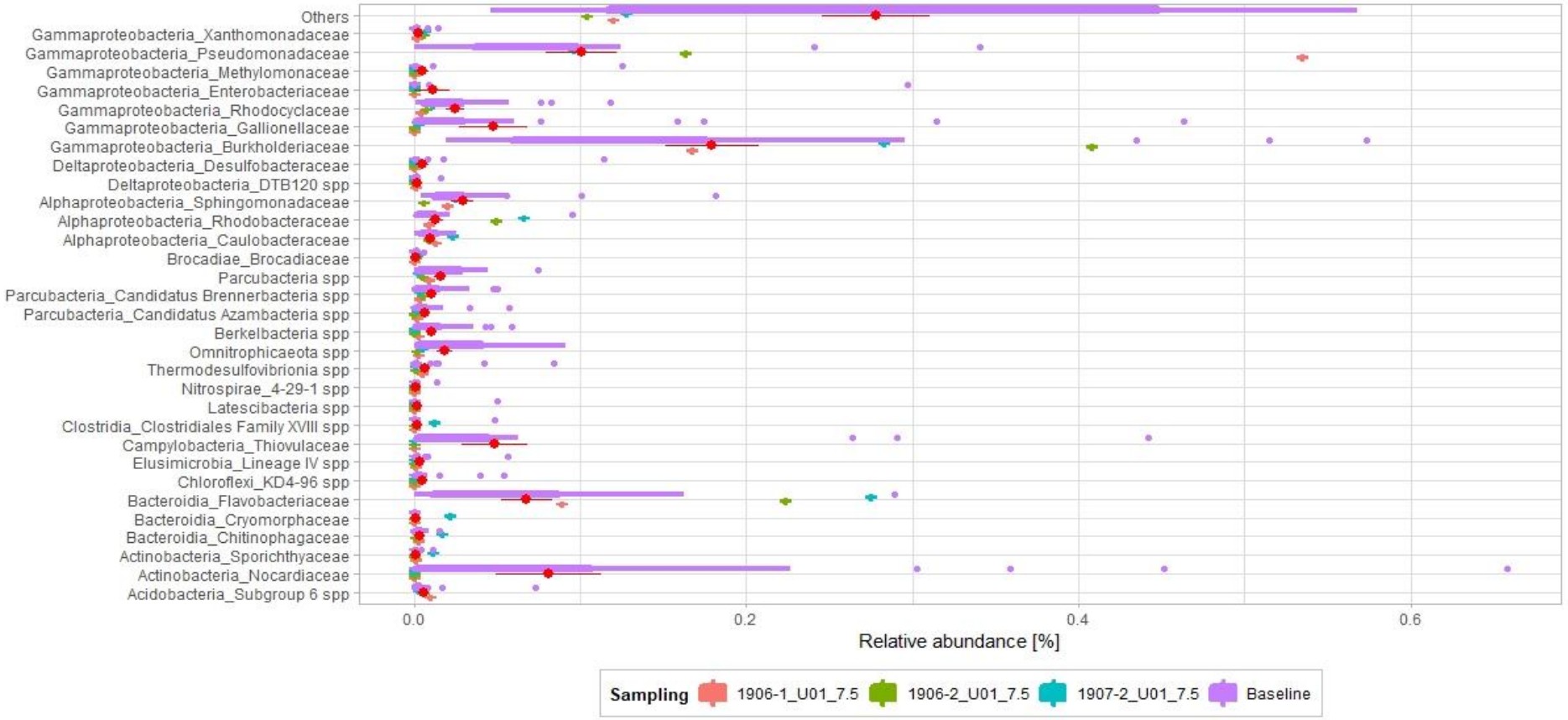


**Figure 2: QIIME2 level 5 results (relative abundances > 5%) for baseline samples as well as for samples from well U01 7.5 m bgs**. Well U01 was the most-heat influenced well that was sampled, reaching temperatures of 35 (1906-1_U01_7.5), 23 (1906-2_U01_7.5), and 16 (1907-2_U01_7.5) °C at this depth 7, 27 – 28, and 62 – 63 days post-infiltration, respectively. Although the groundwater temperature was increased by up to ~ 25 °C, the microbial community composition did not change significantly. The sample IDs are composed of the year of sampling (19 for 2019), the month of sampling (06 for June and 07 for July), the name of the well (U01), and the sampling depth, i. e., 7.5 m bgs. For the baseline samples, the means and standard deviations are illustrated in red.

**Figure 3 (Keller et al.)**

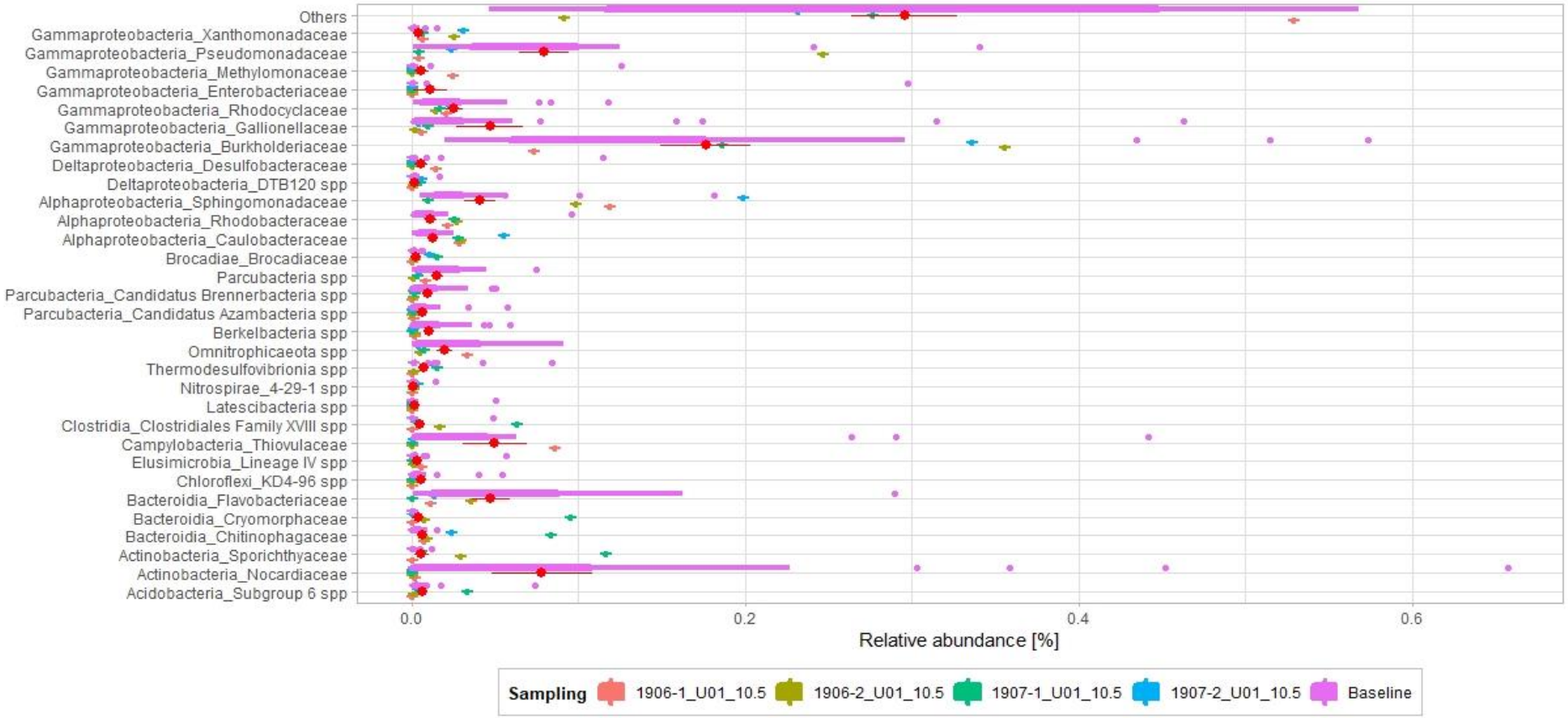


**Figure 3: QIIME2 level 5 results (relative abundances > 5%) for baseline samples as well as for samples from well U01 10.5 m bgs**. Well U01 was the most-heat influenced well that was sampled, reaching temperatures of 31 (1906-1_U01_10.5), 20 (1906-2_U01_10.5), 18 (1907-1_U01_10.5), and 15 (1907-2_U01_10.5) °C at this depth 7, 27 – 28, 40 – 43, and 62 – 63 days post-infiltration, respectively. Major changes in the composition of the microbial community were not observed. The sample IDs are composed of the year of sampling (19 for 2019), the month of sampling (06 for June and 07 for July), the name of the well (U01), and the sampling depth, i. e., 10.5 m bgs. For the baseline samples, the means and standard deviations are illustrated in red.

**Figure 4 (Keller et al.)**

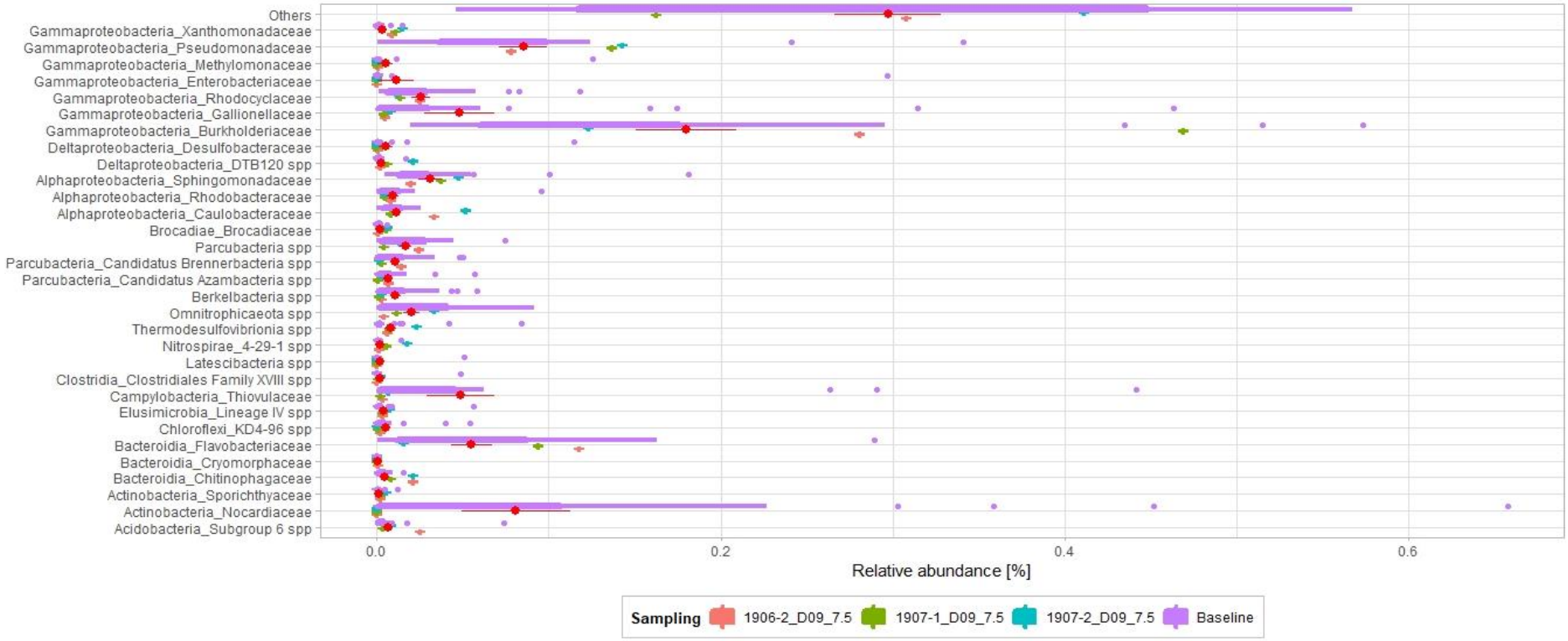


**Figure 4: QIIME2 level 5 results (relative abundances > 5%) for baseline samples as well as for samples from well D09 7.5 m bgs**. The previously heated groundwater flew through well D09, which showed at this depth increased temperatures of 13 (1906-2_D09_7.5), 14 (1907-1_D09_7.5), and 15 °C (1907-2_D09_7.5) 27 – 28, 40 – 43, and 62 – 63 days after the infiltration, respectively. Compared to the baseline samples, the changes in the microbial communities are marginal. The sample IDs are composed of the year of sampling (19 for 2019), the month of sampling (06 for June and 07 for July), the name of the well (D09), and the sampling depth, i. e., 7.5 m bgs. For the baseline samples, the means and standard deviations are illustrated in red.

**Figure 5 (Keller et al.)**

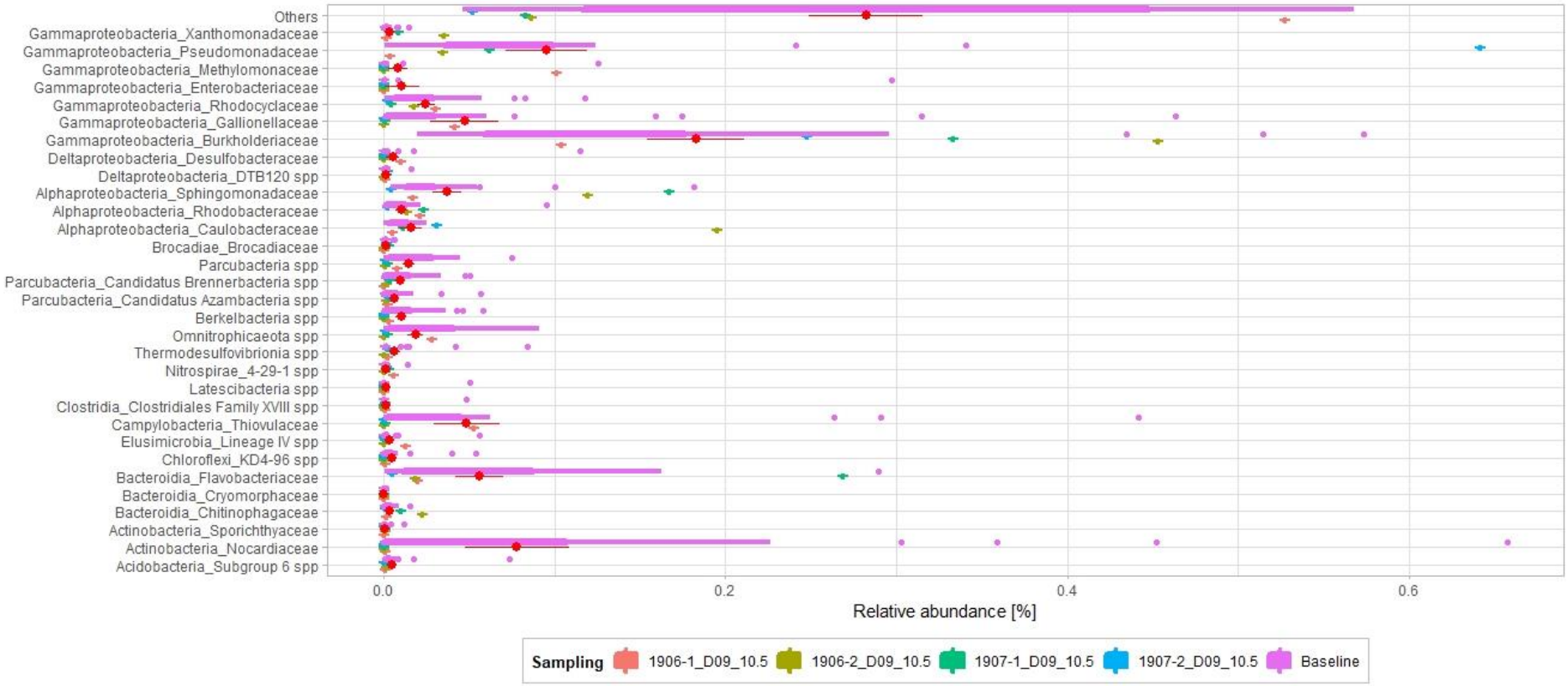


**Figure 5: QIIME2 level 5 results (relative abundances > 5%) for baseline samples as well as for samples from well D09 10.5 m bgs**. The previously heated groundwater flew through well D09, which showed at this depth increased temperatures of 13 °C 62 – 63 days after the infiltration (sample 1907-2_D09_10.5); consistent changes in the microbial community compared to the baseline samples cannot be seen for this sample. The sample IDs are composed of the year of sampling (19 for 2019), the month of sampling (06 for June and 07 for July), the name of the well (D09), and the sampling depth, i. e., 10.5 m bgs. For the baseline samples, the means and standard deviations are illustrated in red.

## Figure 6 (Keller et al.)

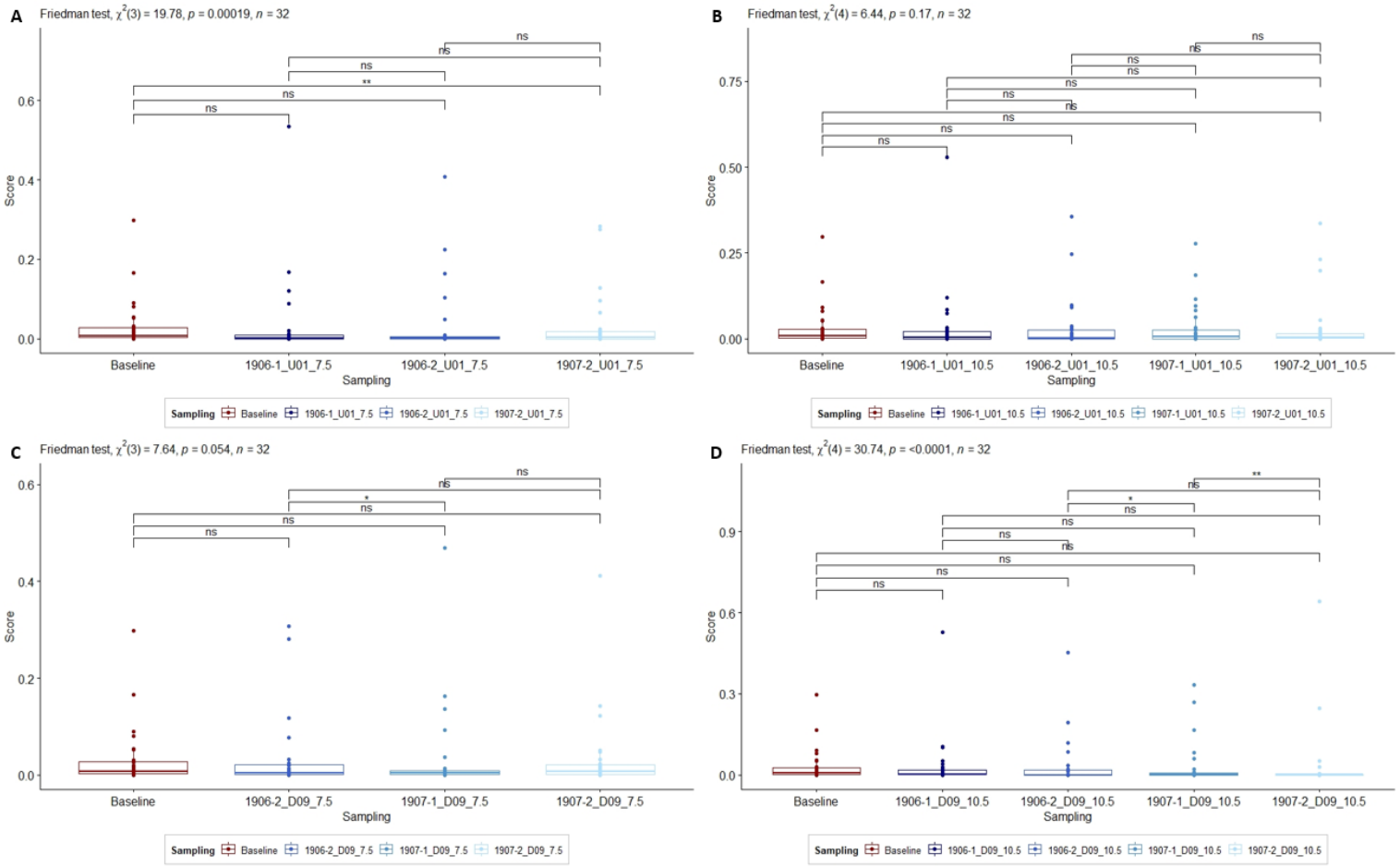


**Figure 6: Boxplots illustrating the results of Friedman tests and Wilcoxon signed-rank tests performed post hoc for baseline samples with samples from well U01 7.5 m (A) and 10.5 m (B) bgs as well as well D09 7.5 m (C) and 10.5 m (D) bgs.** Chi² ($\chi^2$) values (degrees of freedom), p-values, and the number of groups (n) are depicted in each plot (ns – not significant, * – p-value < 0.05, ** – p-value < 0.01). Overall, the microbial communities from baseline samples did not significantly differ from those detected post-infiltration.

**Figure 7 (Keller et al.)**

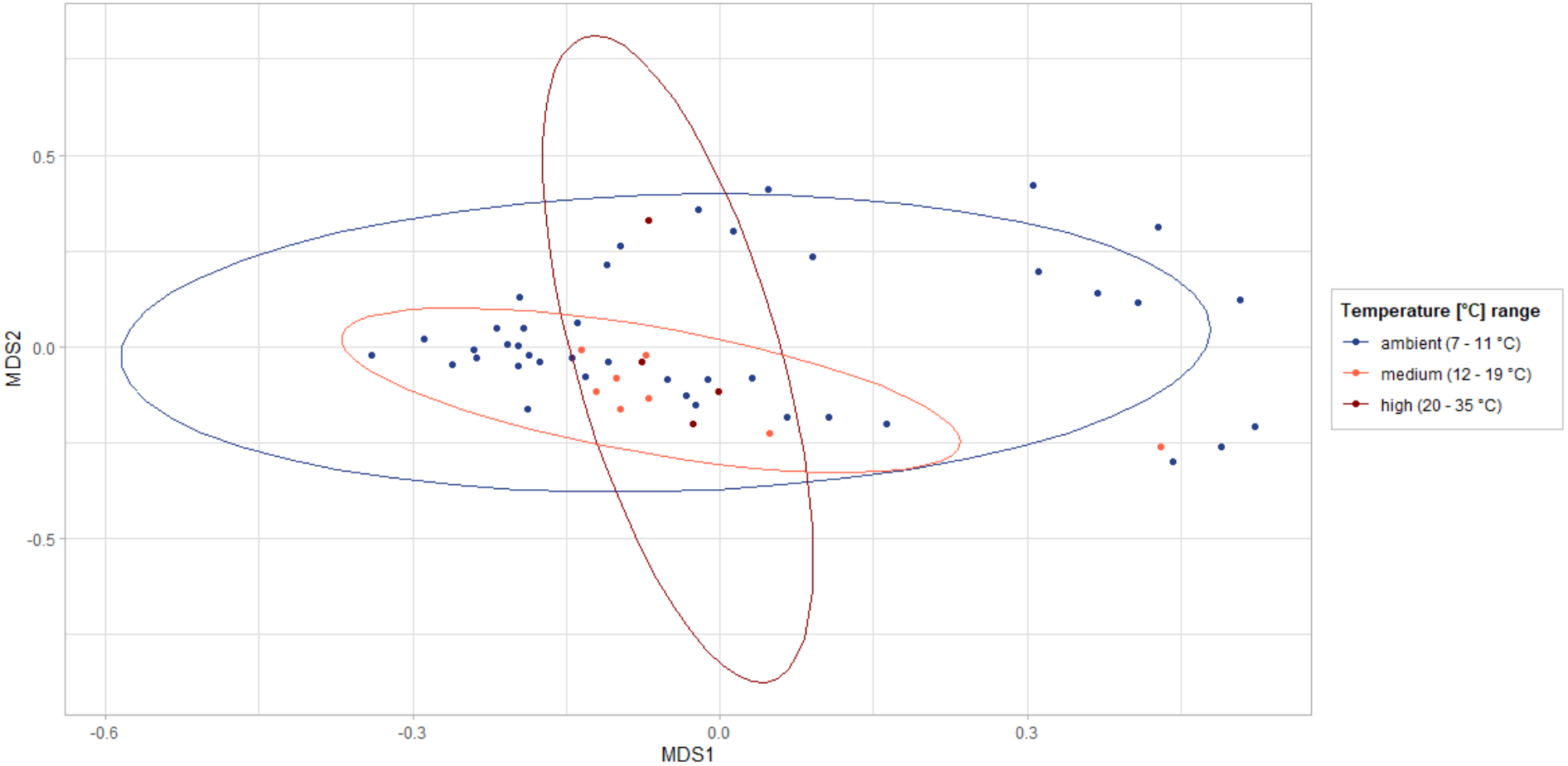


**Figure 7: NMDS plot.** The QIIME2 level 5 results with the temperature as the parameter were used for the NMDS. The results were divided into groups sampled at ambient (7 – 11 °C), medium (12 – 19 °C), and high (20 – 35 °C) groundwater temperatures. The microbial communities detected in the different temperature ranges clustered together.